The Journal of Experimental Biology 204, 2817–2826 (2001)
Printed in Great Britain © The Company of Biologists Limited 2001
JEB3227

AERODYNAMIC STABILITY AND MANEUVERABILITY OF THE GLIDING FROG *POLYPEDATES DENNYSI*

MICHAEL G. McCAY*

University of California – Berkeley, Department of Integrative Biology, Berkeley, CA 94720-3140, USA

*e-mail: mccay@socrates.berkeley.edu

Accepted 29 May 2001

Summary

Gliding has evolved independently in two families of tree frog. Tree frogs glide to descend rapidly to mating sites over temporary pools on the forest floor or to escape predators. The physical mechanisms used by frogs to glide and maneuver were investigated using a combination of observations of live frogs (*Polypedates dennysi*) gliding in a tilted wind-tunnel and aerodynamic forces and torques measured from physical models of tree frogs in a wind-tunnel. Tree frogs maneuvered in the tilted wind-tunnel using two different turning mechanisms: a banked turn (the frog rolls into the turn) and a crabbed turn (the frog yaws into the turn). *Polypedates dennysi* possessed overall weak aerodynamic stability: slightly stable about the pitch and roll axis, slightly unstable about the yaw axis. The maneuverability of gliding tree frogs was quantified using a maneuverability index. The maneuverability of tree frogs was roughly equivalent for tree frogs performing a banked turn and performing a crabbed turn. The maneuverability of tree frogs was approximately one-third of the maneuverability of a falcon (*Falcon jugger*).

Key words: gliding, maneuverability, aerodynamic stability, *Polypedates dennysi*, tree frog.

Introduction

The origin of novel phenotypes has challenged evolutionary biologists since the time of Darwin. Darwin's theory of evolution provides an explanation for how natural selection eliminates the less fit phenotypes, but leaves open the question of how novel phenotypes arise. The origins of animal flight are particularly important evolutionary transitions because aerial locomotion is thought to be a significant factor in the diversification of birds (Padian and Chiappe, 1998), bats (Thewissen and Babcock, 1992) and insects (Kingsolver and Koehl, 1994; Carpenter and Richardson, 1985; Wootton, 1981). The rigorous evaluation of any hypothesis of the origin of flight requires a comparative study between basal non-flying species and derived flying species. Among the birds and bats, two of the most famous and capable flying vertebrate lineages, the only non-flying species available for study are either extinct fossils or extant species that have secondarily lost the ability to fly, such as penguins or ostriches.

Gliding frogs

Gliding originated independently within two families of tree frogs, the Hylidae and the Rhacophoridae (Emerson and Koehl, 1990). Within each evolutionary lineage are extant species spanning the full range of gliding abilities: non-gliding species, intermediate species and gliding species (Duellman, 1970; Emerson and Koehl, 1990). Therefore, tree frogs present an excellent system in which to study the origin of gliding because they are living, behaving organisms that possess a range of gliding abilities that can be directly observed and compared.

Gliding tree frogs of both families share a suite of morphological features (e.g. enlarged, extensively webbed hands and feet, skin flaps on elbows and ankles) and use similar limb postures while gliding (Emerson and Koehl, 1990; M. G. McCay, personal observations). These frogs use gliding to descend from the canopy down to mating sites over temporary pools on the rainforest floor (Roberts, 1994) and to escape from predators (Emmons and Gentry, 1983). Emerson et al. (Emerson et al., 1990) compared the gliding performance of gliding frogs with that of non-gliding frogs and found that the morphological features and limb postures of the gliding frogs were associated with higher gliding distances and much greater maneuverability.

Aerodynamic stability and maneuverability

Animal flight is a complex interaction between aerodynamic forces and torques, the animal's mass properties and the behavior of the animal. The motion an animal experiences during flight is marked by transitory oscillations (phugoid mode, short-period mode, Dutch-roll mode and spiral mode) superimposed over translation along a flight path (McCormick, 1976). In addition, the flight path may be changing as a result of postural changes by the animal.

Maneuverability is the ability of a gliding animal to accelerate and change its flight path. In general, a gliding

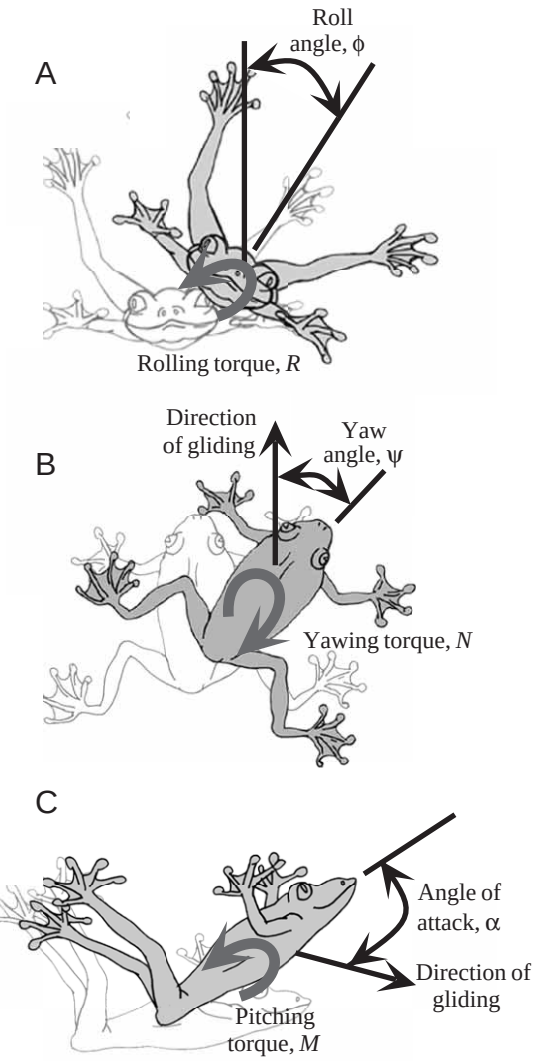

Fig. 1. Rotation angles. Rotation about the frog's center of mass can be resolved into rotations about three orthogonal axes. The origin of the axes is fixed to the animal's center of mass, and the axes themselves are fixed to the animal; the axes translate and rotate as the animal translates and rotates. (A) Rotation about the cranial–caudal axis is termed roll angle, ϕ; rolling rotates the animal's right side up or down. (B) Rotation about a dorso-ventral axis is termed yaw angle, ψ; yawing rotates the animal's snout to the left or right. (C) Rotation about a lateral axis is termed angle of attack, α; pitching rotates the animal's snout up or down. Grey arrows indicate the directions of the indicated torques.

animal is capable of accelerating linearly (such as slowing down) and rotationally (such as twisting around the cranial–caudal axis). Here, I will examine turning, or changing the animal's direction of gliding. Turning maneuvers are accomplished by rotations about the glider's center of mass that in turn alter the aerodynamic forces acting on the glider. This rotation can be resolved into rotations about three orthogonal axes, pitch, roll and yaw, as shown in Fig. 1. Maneuverability depends on the magnitude of the aerodynamic forces the frog can generate as well as the frog's aerodynamic stability.

Aerodynamic stability is the ability of a gliding animal to maintain its flight path in the presence of perturbations. When perturbed from some initial position, a gliding animal that is aerodynamically stable will return passively to its original position, much like a weathervane aligns itself passively with the wind. Thus, aerodynamic stability is a passive interaction between a gliding animal's morphology and the surrounding airstream that allows an animal to maintain its direction of flight without actively steering to control its direction of flight.

A gliding animal experiences many transitory oscillations in the course of gliding. If an animal is dynamically stable, these oscillations will damp out in the absence of any behavioral control on the part of the animal. If the animal is dynamically unstable, these oscillations will grow in magnitude unless the animal actively steers to counteract the oscillations. Dynamic stability depends on both the mass properties of the animal and its aerodynamic properties, including aerodynamic stability (McCormick, 1976). The more aerodynamically stable a gliding animal is, the more likely that the animal will be dynamically stable (McCormick, 1976).

Aerodynamic stability can be quantified as the change in aerodynamic torque per unit rotation about an axis (i.e. the slope of the graph of aerodynamic torque plotted as a function of rotation angle) (McCormick, 1976). Fig. 2 shows a hypothetical plot of the change in pitching torque as a function of angle of attack for a stable frog (Fig. 2A), a neutrally stable frog (Fig. 2B) and an unstable frog (Fig. 2C). A linear regression through the pitching torque data as a function of angle of attack is used to assess the stability of the frog about its pitch axis. The examples shown in Fig. 2 intersect the horizontal axis (angle of attack) at the equilibrium point, the angle at which no aerodynamic torque acts to rotate the frog; the frog naturally glides at the angle of attack corresponding to the equilibrium point.

In Fig. 2A, if the frog's angle of attack is perturbed in a nose-up direction, an aerodynamic torque is induced that rotates the frog in a nose-down direction, back towards equilibrium. If the frog is perturbed in a nose-down direction, an aerodynamic torque is induced that rotates the frog nose-up, back towards equilibrium. A frog with these aerodynamic characteristics is aerodynamically stable.

The slope of the linear regression of aerodynamic torque about the pitch axis *versus* angle of attack determines the level of aerodynamic stability that the frog possesses about the pitch axis. A steep negative slope indicates that a large restoring torque would be induced for a small change in angle, so the frog would be highly stable. A flatter negative slope indicates weaker stability because a smaller restoring torque would be induced for a change in angle. Zero slope (a horizontal line) (Fig. 2B) indicates neutral stability because torque would not change with angle, no restoring torque would be induced and the frog would remain at the angle to which it was perturbed. A positive slope (Fig. 2C) indicates an unstable frog, since any perturbation in angle of attack away from the equilibrium point induces a torque that would rotate the frog further away from the equilibrium point.

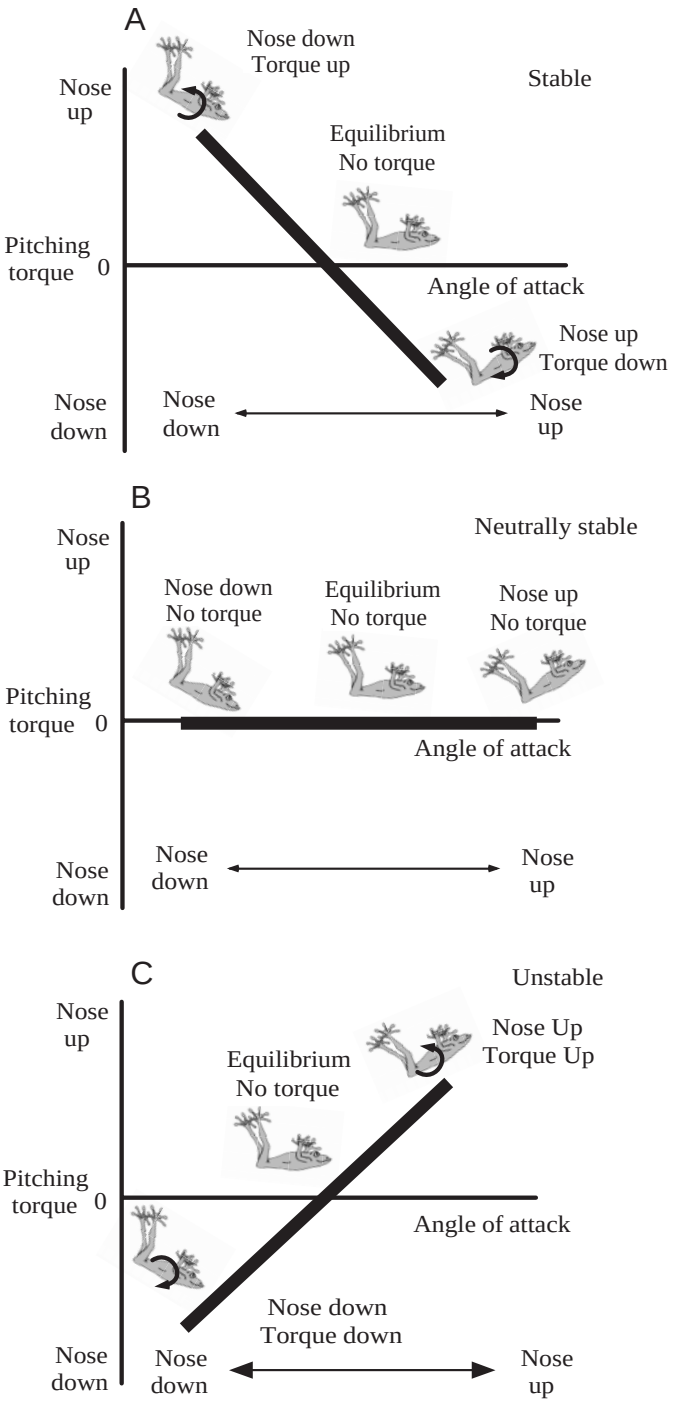

Fig. 2. Aerodynamic stability determined by the slope of measured aerodynamic torque about a rotational axis (here pitch) plotted as a function of the angular orientation about the same rotational axis. (A) Measured aerodynamic torques about the pitch axis for an aerodynamically stable frog. At the equilibrium angle of rotation, no torques are acting on the frog, so it remains at equilibrium. If a gust of wind pitches the frog's nose away from its initial position in either the upward or downward direction, this change in orientation relative to the airflow induces an aerodynamic torque that tends to rotate the frog back to its initial position. (B) Measured aerodynamic torques for a neutrally stable frog. If a gust of wind pitches the frog's nose away from its initial position in either the upward or downward direction, this change in orientation relative to the airflow induces no aerodynamic torque that tends to rotate the frog back to its initial orientation or to rotate the frog further away from its initial orientation, so the frog remains at the angular orientation to which it was pitched. (C) Measured aerodynamic torques for an aerodynamically unstable frog. If a gust of wind pitches the frog's nose away from its initial position in either the upward or downward direction, this change in orientation relative to the airflow induces an aerodynamic torque that tends to rotate the frog even further away from its initial position, causing the frog to diverge from its original flight path.

A potential trade-off exists between aerodynamic stability and maneuverability (Maynard Smith, 1952); aerodynamic stability minimizes the effect of random perturbations (such as wind gusts), but aerodynamic stability also counteracts intentional perturbations performed by the animal (such as the initiation of turns). A gliding animal that is aerodynamically stable has a more sluggish initial response to a steering motion than does a gliding animal that is aerodynamically unstable. Therefore, an aerodynamically stable frog must execute a steering motion much more forcefully to accomplish the same maneuver in the same amount of time as an aerodynamically unstable frog. However, a gliding animal that is aerodynamically unstable requires more active steering to maintain its direction of flight than does an animal that is aerodynamically stable because each wind gust that hits the animal causes it to veer off course unless the animal actively executes a steering motion to get itself back on course.

Thus, if a gliding frog is airborne and a wind gust disturbs the animal from its intended path, the animal can regain its original flight path in one of two ways: (i) it can change its posture and actively steer itself back on course, or (ii) if the frog is aerodynamically stable, it can remain in the same fixed posture and let its aerodynamic stability return it back on course. The presence or absence of aerodynamic stability directly affects the amount of corrective steering required to glide successfully.

Although aerodynamic stability and maneuverability are central issues in animal flight, few investigators have actually measured the aerodynamic stability and maneuverability of animals (Harris, 1936). Once stability and maneuverability have been measured, meaningful assessments of the trade-off between stability and maneuverability can be made. In addition, once stability and maneuverability have been well characterized, assessments of the behavioral control of flight may also be performed. However, before assessing the trade-off between stability and maneuverability, one must first understand the basic physical mechanisms used by tree frogs to glide and maneuver.

Objectives

The purpose of this study was to determine how tree frogs glide and maneuver by observing the behavior of live gliding tree frogs. The specific questions addressed were as follows. (i) What physical mechanisms do gliding frogs use to

accomplish maneuvers? (ii) Are gliding frogs aerodynamically stable or unstable? (iii) How maneuverable are gliding frogs compared with other gliding animals? A thorough understanding of the aerodynamic issues associated with gliding provides a solid foundation from which to investigate the evolution of gliding in tree frogs.

Materials and methods

Frog care and handling

Adult *Polypedates dennysi* (Blanford) were collected from the Tham Dao nature preserve in northern Vietnam and transported to the animal care facility at UC-Berkeley. *Polypedates dennysi* (from the anuran family Rhacophoridae) is a gliding tree frog that inhabits rain forests throughout southeast Asia and possesses enlarged, extensively webbed hands and feet. The frogs (N=3) were kept in a climate-controlled room at 26 °C, 75 % humidity on a photoperiod of 12 h:12 h L:D. Each frog was kept in a separate container, fed 3–5 crickets daily, and given water *ad libitum*. The frogs were weighed, and snout–vent length was measured before and after each session in the wind-tunnel. The three frogs tested weighed 61.9–62.4 g, 68.5–70.2 g and 99.2–100.8 g and measured 97.6–98.1 mm, 104.2–105.1 mm and 108.5–111.0 mm snout–vent length respectively. Frogs were misted with water after each wind-tunnel run to maintain hydration. All experiments using living frogs were performed with the prior approval of the Animal Care and Use Committee of the University of California at Berkeley.

Maneuvers with a stimulus

Gliding conditions were simulated using a tilted wind-tunnel similar in design to tilted wind-tunnels used previously to study the flight of birds (Pennycuick, 1968; Tucker and Heine, 1990). When a frog glides through the air, the airflow with respect to the frog is parallel to the frog's flight path, but in the opposite direction from that in which the frog is moving (see Fig. 3A). The airflow past a frog that is gliding in the working section of the tilted wind-tunnel simulates the airflow relative to a frog gliding through still air (see Fig. 3B). Tree frogs glide through the air on an inclined path; the angle that the frog's glide path makes with respect to the ground is the frog's glide angle (see Fig. 3A). In addition, a gliding frog's entire body is inclined relative to its glide path; the angle between the frog's body (snout-to-vent line) and its glide path is the frog's angle of attack (see Fig. 3A).

A glide angle of 45 ° was used in the tilted wind-tunnel in this study, corresponding to glide angles observed from videotaped glides of frogs in open air filmed in the laboratory. Airspeeds were set to a level (between 12 and 14 m s^{-1}) that suspended the frogs in the tunnel's airflow with no rising or falling movement; this airspeed range corresponded to a Reynolds number range from 75 000 to 100 000 for the frogs. Larger, heavier frogs required higher airspeeds (14 m s^{-1}) to generate the higher aerodynamic forces required to simulate gliding in open air. All wind-tunnel runs were performed at room temperature (24–27 °C).

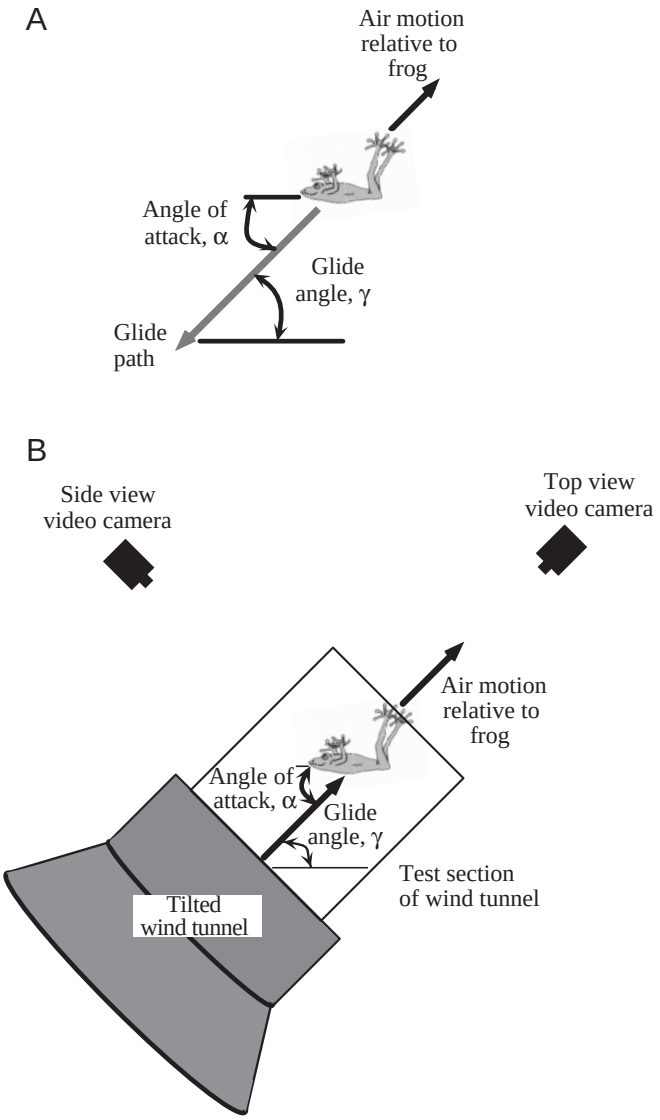

Fig. 3. (A) A frog gliding through the air; the airflow with respect to the frog is parallel to the frog's flight path, but in the opposite direction from that in which the frog is moving. The angle of the frog's glide path with respect to the horizontal is called the glide angle, γ. The angle that the frog's cranial–caudal axis makes with the frog's glide path is called the angle of attack, α. (B) If a wind-tunnel is tilted to the glide angle of a frog, the airflow past a frog that is stationary in the working section of the wind-tunnel simulates the airflow relative to a frog gliding at that angle through still air. Air is blown by a 560 W fan through the transparent test section of the wind-tunnel, measuring 38 cm high, 38 cm wide and 46 cm long. The tunnel can be tilted to blow air at any orientation ranging from vertical to horizontal. The tunnel airspeed was continuously adjustable up to 18 m s^{-1}. Observations of *Polypedates dennysi* gliding in free air and in the wind-tunnel show that this species glides at a glide angle of 45 ° and an airspeed of approximately 13 m s^{-1}.

The tilted wind-tunnel used for these experiments had a

transparent Plexiglas test section through which the frogs were videotaped. Airspeed was controlled using a variable-resistance rheostat (Powerstat type 3PN116, The Superior Electric Company, Bristol, CT, USA) that controlled airspeed over the range 0–18 m s^{-1}. The wind-tunnel had a contraction ratio of 3.4 and a turbulence intensity of less than 1 % over the full range of tunnel speeds, as measured using a hot-wire anemometer (Kurz air velocity meter, model 443M). The test section had a safety net installed to prevent accidental movement of a frog into the expansion chamber of the wind-tunnel.

The stimulus used to induce a frog to turn was a plastic plant similar to plastic plants kept in each frog's living quarters. The plant was stuck to the outside of the wind-tunnel test section so that it was visible to the frog but did not change the airflow within the test section. The stimulus treatments used were (i) no plant (control), (ii) plant on the left side of the test section, and (iii) plant on the right side of the test section. Each frog was exposed to each of the stimulus treatments 20 times. All treatments for all frogs were used on each of two days, with the order of individual frogs and treatments determined using a random number table.

During a wind-tunnel run, the plant stimulus was put into place, and the frog was removed from its container and released into the tunnel test section. The frog was released at an angle of attack of approximately 45 °, with its mid-sagittal plane parallel with the direction of airflow (i.e. zero yaw angle). The frog's motion and behavior during each wind-tunnel run were videotaped from above and from the side (see Fig. 3B) using video camcorders (Sony Hi-8 video camera recorders CCD-V9 and CCD-TR101) at a rate of 60 frames s^{-1}.

The videotaped wind-tunnel runs were examined to determine maneuvering behavior. A run was scored as a turning maneuver if the frog's final snout orientation had changed in yaw angle by more than 60 °. Maneuvers were scored as (i) left turn, (ii) no turn or (iii) right turn.

Posture during maneuvers

Videotapes from the wind-tunnel runs described above were analyzed to identify changes in the frog's posture while turning. The positions of a frog's arms and legs were noted, and the movements of these limbs were qualitatively determined in three directions: forward–aft (cranial–caudal), towards and away from the center line of the body (lateral), and above or below the plane of the body (dorsal–ventral). Selected runs were analyzed in the Peak Motus 3-D motion-analysis system to acquire the three-dimensional coordinates of the frog's appendages with respect to its center of mass; the calculated coordinates were used to verify the qualitative observations of limb postures from the selected runs. Limb postures and motions qualitatively observed when frogs executed turns were compared with those observed when frogs were gliding without turning to identify behaviors that were potentially involved in maneuvering.

Three-dimensional kinematic analysis of turns

Wind-tunnel runs were identified from videotape where (i) the frog was centered in the wind-tunnel test section with no yaw angle when first released into the test section, and (ii) the frog moved from the center of the test section to the test section wall on the frog's left or right. These videotaped wind-tunnel runs were used in a three-dimensional motion analysis to determine the frog's rotations while maneuvering. The videotapes were analyzed in the Peak Motus 3-D motion-analysis system to acquire the three-dimensional coordinates of the frog's body features throughout the course of a maneuver. These three-dimensional coordinates were used to calculate the frog's rotation about the pitch, yaw and roll axes during the course of a maneuver. Changes in pitch and roll angles with respect to the horizontal plane and changes in yaw angle with respect to the direction of airflow in the test section were calculated. These angles were compared between wind-tunnel runs to determine whether any differences in angular orientations during a turn were associated with a particular posture.

Stability of gliding frogs

Torques acting on *Polypedates dennysi* were measured using a full-scale physical model of the frog in the wind-tunnel. The model was fabricated by making an impression of a preserved adult *Polypedates dennysi* specimen in dental alginate (Jeltrate alginate impression material, Dentsply International Inc.), then casting the frog model in flexible silicone (LS-40 silicone rubber, BJB Enterprises, Inc.) with a rigid wire skeleton inside. The frog model was posed in a fixed posture corresponding to the posture used by the live gliding frogs in the tilted wind-tunnel. The frog model was mounted on an instrumented balance that measured the torque acting about the model's center of mass.

Torques were measured about the pitch axis at angles of attack of 0, 20, 30, 45, 60 and 90 °. Each series from 0 to 90 ° was repeated five times. Similar series were run to measure torques about the roll axis and yaw axis for roll (and sideslip) angles of 90, 60, 45 and 30 ° to the left and 0, 30, 45, 60 and 90 ° to the right.

As described above, the slope of the linear regression of the aerodynamic torque plotted as a function of rotation angle determines the aerodynamic stability. To compare the aerodynamic stability of *Polypedates dennysi* with that of other gliding animals, the effects of the frog's physical size and airspeed must be removed from the stability slopes described above. The effects of size and airspeed were removed from the stability slopes by dividing these slopes by the frog's planform area (the projected area of the frog as seen from above), its snout–vent length (the distance from the tip of the frog's snout to its cloacal opening) and the dynamic pressure (the portion of the total energy of a moving fluid due to kinetic energy) (Vogel, 1994) at which the torque data were measured in the wind-tunnel, yielding three dimensionless stability coefficients (McCormick, 1976).

The stability slopes were divided by snout–vent length,

rather than wing chord length or wing span, because snout–vent length was an easily measured physical length of a frog that does not change when the frog assumes different postures. In addition, snout–vent length is of the same order of magnitude with respect to overall size as wing chord length and wing span, so the absolute values of the stability coefficients will be consistent with those of other animals and/or aircraft.

The stability coefficients defined below are analogous to the dimensionless lift coefficient (C_L) and drag coefficient (C_D) used in other fluid dynamic analyses (Vogel, 1994). The conventions and notations used to define the stability coefficients are taken from aircraft stability and control theory (McCormick, 1976).

Rolling stability coefficient $C_{r,\phi}$

$$C_{r,\phi} = \frac{\partial C_r}{\partial \phi}, \quad (1)$$

where ϕ is the roll angle (rad) and C_r is the rolling moment coefficient:

$$C_r = \frac{R}{qS\lambda}, \quad (2)$$

where R is the rolling torque (N m), S is the reference planform area (m^2), λ is the snout–vent length (m) and q, the dynamic pressure ($N\,m^{-2}$), is:

$$q = \tfrac{1}{2}\rho V^2, \quad (3)$$

where ρ is the density of air ($kg\,m^{-3}$) and V is the frog's airspeed ($m\,s^{-1}$). Roll angle ϕ and rolling moment R are drawn in Fig. 1A; ϕ and R are defined as positive in the direction that rotates the frog's right lateral side down (McCormick, 1976).

In engineering literature, wing span is used in place of λ in equation 2. In addition, rolling moment has previously been assigned the symbol L (McCormick, 1976); I use the symbol R to avoid confusion with aerodynamic lift, which also uses the symbol L.

Pitching stability coefficient $C_{m,\alpha}$

$$C_{m,\alpha} = \frac{\partial C_m}{\partial \alpha}, \quad (4)$$

where α is angle of attack (rad) and the pitching moment coefficient C_m is:

$$C_m = \frac{M}{qS\lambda}, \quad (5)$$

where M is the pitching torque (N m). Pitching torque M and angle of attack α are drawn in Fig. 1C; M and α are defined as positive in the direction that rotates the frog's nose upwards (McCormick, 1976). In engineering literature, wing chord length is used in place of λ (McCormick, 1976).

Yawing stability coefficient $C_{n,\psi}$

$$C_{n,\psi} = \frac{\partial C_n}{\partial \psi}, \quad (6)$$

where ψ is the yaw angle (rad) and the yawing moment coefficient C_n is:

$$C_n = \frac{N}{qS\lambda}, \quad (7)$$

where N is the yawing torque (N m). Yawing torque N and yaw angle ψ are drawn in Fig. 1B; N and ψ are defined as positive in the direction that rotates the frog's nose to the right (McCormick, 1976). In engineering literature, sideslip angle is used in place of yaw angle and wing span is used in place of λ.

The sign of the slope of the measured torque *versus* angle will determine whether or not the frog is stable. Because the torque and angle are defined as positive in the same direction for pitch, roll and yaw, a negative stability coefficient indicates aerodynamic stability. A positive stability coefficient indicates aerodynamic instability, and a stability coefficient of zero indicates neutral stability.

Maneuverability of gliding frogs

Using aerodynamic forces measured from a full-scale physical model in the wind-tunnel, the maneuverability of different turns can be compared. The same physical model of *Polypedates dennysi* used to measure aerodynamic torques above was used for the aerodynamic force measurements. The frog model was mounted on a device that measured the aerodynamic force acting on the model in a single direction, and force measurements were taken using a similar protocol to the aerodynamic torque measurements described above.

Fig. 4 illustrates the aerodynamic forces that describe the frog's ability to turn for two types of turn: banked turns and crabbed turns. These two types of turn represent two different turning strategies that utilize different physical mechanisms to achieve a turn. In a banked turn (Fig. 4A), the frog rolls into the turn. The banking frog's lift force vector is tilted towards the center of the turn because of the frog's roll angle. The component of the lift force acting towards the center of the turn is the centripetal force that pulls the frog through the turn. In a crabbed turn (McCormick, 1976), the frog yaws into the turn (Fig. 4B). By yawing, the frog induces a sideways-directed force that acts towards the center of the turn. This force is the centripetal force that pulls the frog through the turn.

Lift force was measured at angles of attack of 0, 20, 30, 45, 60 and 90°, and centripetal force was measured at yaw angles of 0, 15 and 30° to the left and 15 and 30° to the right.

One way to quantify maneuverability is to assess how much centripetal turning force can be generated for a given change in rotation angle. To generate the centripetal force necessary to turn at a desired rate, how far does one need to rotate? The higher the centripetal force per degree of rotation, the more responsive the frog will be to rotations (banking or

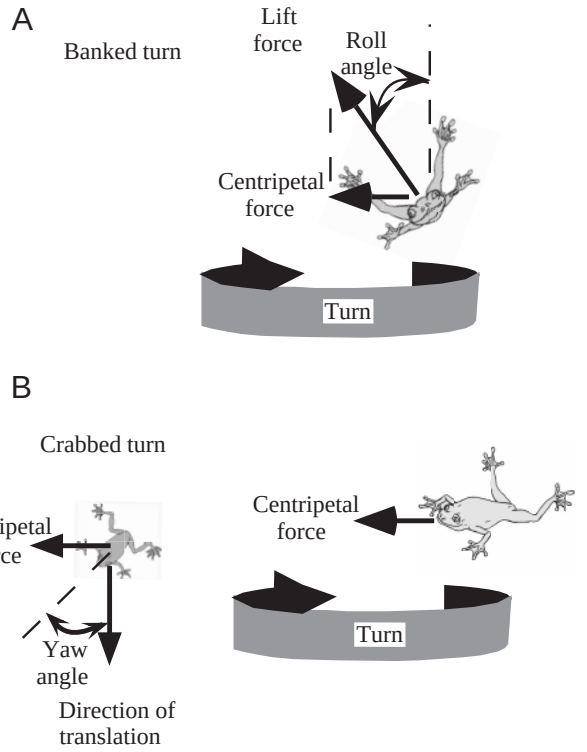

Fig. 4. Diagram showing two types of turning technique. (A) A 'banked turn', during which the frog rolls into the turn. By rolling, the frog tips the direction of the lift force towards the center of the turn; the sideways component of lift pulls the frog through the turn. (B) A 'crabbed turn', during which the frog yaws into the turn; airflow asymmetries on the frog's left and right sides induce a centripetal force that pulls the frog through the turn.

yawing), and therefore the more maneuverable the frog will be. For crabbed turns, the change in centripetal force F_c per change in yaw angle ($\partial F_c/\partial\psi$) is given by the slope of the linear regression through the measured centripetal force data (in the engineering literature, 'side force') plotted as a function of yaw angle. For banked turns, the maximum turning force for a given roll angle is achieved at the maximum lift force:

$$F_c = L_{max}\sin\phi\,, \tag{8}$$

where F_c is centripetal force (N), L_{max} is maximum lift force (N) and ϕ is roll angle (rad).

The change in turning force per unit angle in a banked turn is given by:

$$\frac{\partial F_c}{\partial\phi} = L_{max}\cos\phi\,. \tag{9}$$

The change in turning force for crabbed turns is a function of yaw angle (ψ) and must be directly measured.

To compare maneuverability between different animals, the effects of the animal's weight must be removed from the slopes given above ($\partial F_c/\partial\psi$ for crabbed turns, $\partial F_c/\partial\phi$ for banked turns). The slopes given above divided by the animal's weight W yields a dimensionless index of maneuverability (I_m).

For crabbed turns:

$$I_m = \frac{1}{W}\frac{\partial F_c}{\partial\beta}\,. \tag{10}$$

For banked turns:

$$I_m = \frac{1}{W}\frac{\partial F_c}{\partial\phi}\,. \tag{11}$$

Results

Maneuvering mechanisms of gliding frogs

The frequencies of turning behaviors for each stimulus treatment (plant to left, no plant or plant to right) for each frog are shown in Fig. 5. The frequencies are calculated as a percentage of the total turning behaviors observed for a given stimulus treatment. The turning behavior of all three frogs changed significantly in the presence of the plant stimulus, although the direction of change was inconsistent between frogs. Frog 1 turned more away from the plant stimulus, and frogs 2 and 3 turned more towards the plant stimulus. These data demonstrate that *P. dennysi* does maneuver in response to the stimulus provided.

The frequencies of the frog's postures while turning to the left, going straight or turning right are shown in Fig. 6 for each of the three frogs. The frequencies are expressed as a percentage of the total observations of a given maneuver. All three frogs exhibit similar postures when turning, namely the foot opposite to the turn is held higher. For example, in a turn towards the left, the frog's right foot was held higher. However, for 35 % of the observed turns, the feet were held at equal heights. These two postures correspond to the two different turning techniques used by *Polypedates dennysi*.

Pitch, roll and yaw angles during two turns to the left are shown in Fig. 7: a banked turn with the feet held at equal heights (Fig. 7A) and a crabbed turn with the right (opposite) foot held higher (Fig. 7B). Pitch angle is relatively constant and equal to approximately 60 ° for both turns shown. Yaw angle changes by the same magnitude (80 °) at approximately the same rate (400 ° s^{-1}) for both turns. However, roll angle differs between the two turns, covering approximately 60 ° for the banked turn and 0 ° for the crabbed turn.

Aerodynamic stability of gliding frogs

The torques acting on a full-scale physical model of *P. dennysi* in a wind-tunnel are shown in Fig. 8A–C. Stability coefficients are shown in Fig. 8D. The frog is slightly stable about the pitch and roll axes and is slightly unstable about the yaw axis.

Maneuverability of gliding frogs

The maneuverability index for the gliding frog performing a banked turn is 6.1×10^{-5} to 1.1×10^{-4} rad^{-1} and for a crabbed turn is 5.4×10^{-5} to 8.2×10^{-5} rad^{-1}. In contrast, the maneuverability index calculated for a falcon *Falco jugger*

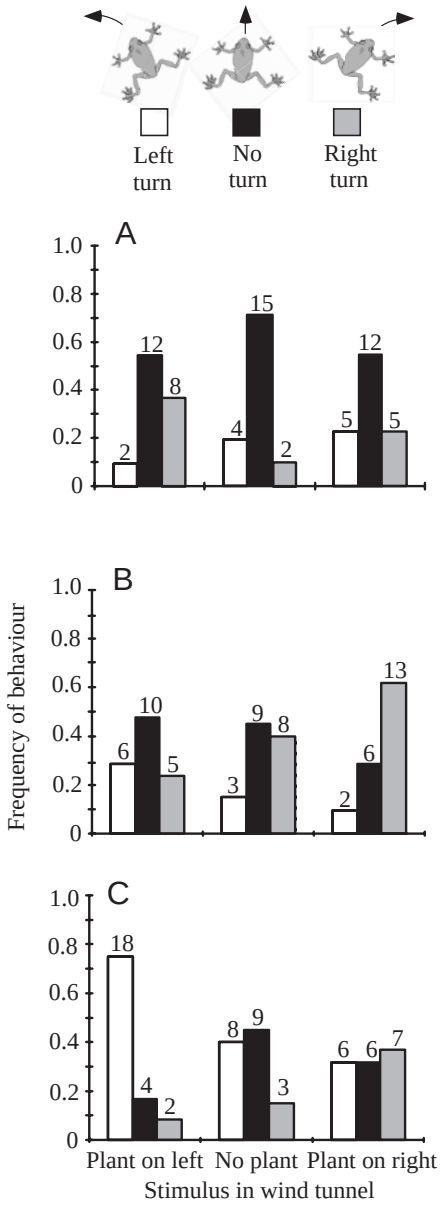

Fig. 5. Turning behavior of frogs. Frequency of left turns (open columns), no turns (black columns) and right turns (grey columns) in the presence of a visual stimulus are shown for three *Polypedates dennysi* frogs in a wind-tunnel. All frogs maneuvered significantly more in the presence of the stimulus. (A) Frog 1; this frog turned significantly more often away from the plant (χ^2-test, P=0.02). (B) Frog 2; this individual turned significantly more often towards the plant (χ^2-test, P=0.01). (C) Frog 3; this individual turned significantly more often towards the plant (χ^2-test, $P \ll 0.001$). Numbers of actual occurrences of each maneuver are shown above each column on the graphs.

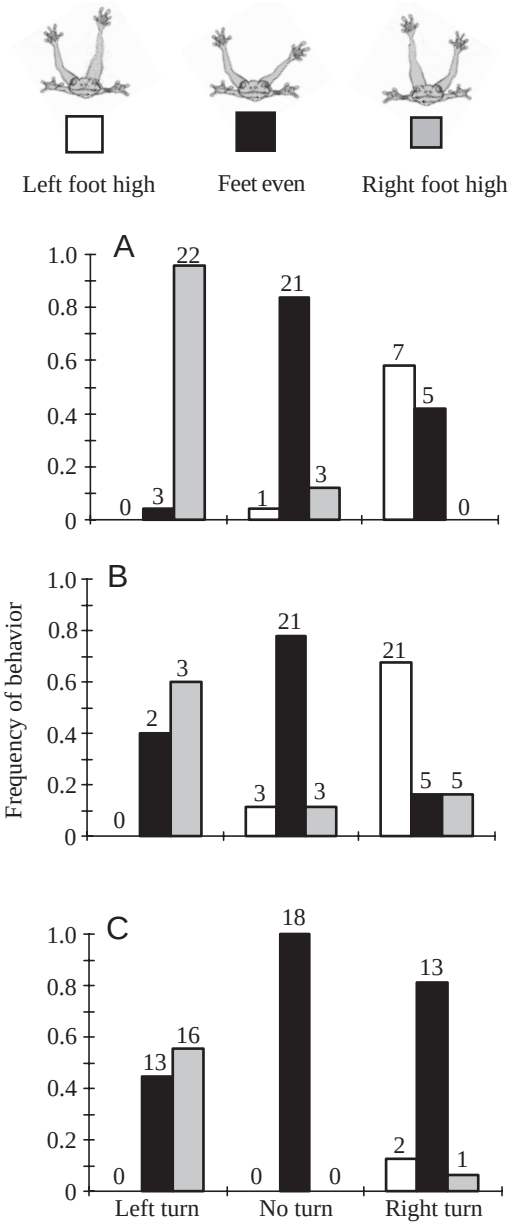

Fig. 6. Foot position during maneuvers. Frequencies of the indicated foot positions for frog 1 (A), frog 2 (B) and frog 3 (C) are shown for left turns, straight gliding without a turn and right turns. Absolute numbers of occurrences of a behavior are shown above the columns. All frogs show significant changes in foot position while turning relative to their foot positions when gliding straight without turning (χ^2-test, $P \ll 0.001$). All frogs held the foot opposite to the direction of the turn higher; the left foot was held higher during right turns, and the right foot was held higher during left turns.

from data in Tucker and Parrott (Tucker and Parrott, 1970) is 1.8×10^{-4} to 3.3×10^{-4} rad^{-1}. The maneuverability index for a banked turn is slightly higher than the maneuverability index for a crabbed turn. Both the banked and crabbed turns of the gliding frog have lower maneuverability than the maneuverability of a falcon performing a banked turn.

Discussion

Turning techniques: banked turns versus *crabbed turns*

Polypedates dennysi utilize two different techniques to turn: banked turns and crabbed turns. The banked turn until now has been the only mechanism used to describe turning in animal flight (Pennycuick, 1972; Norberg, 1994). Previous studies of gliding frog aerodynamics assumed a banked turning

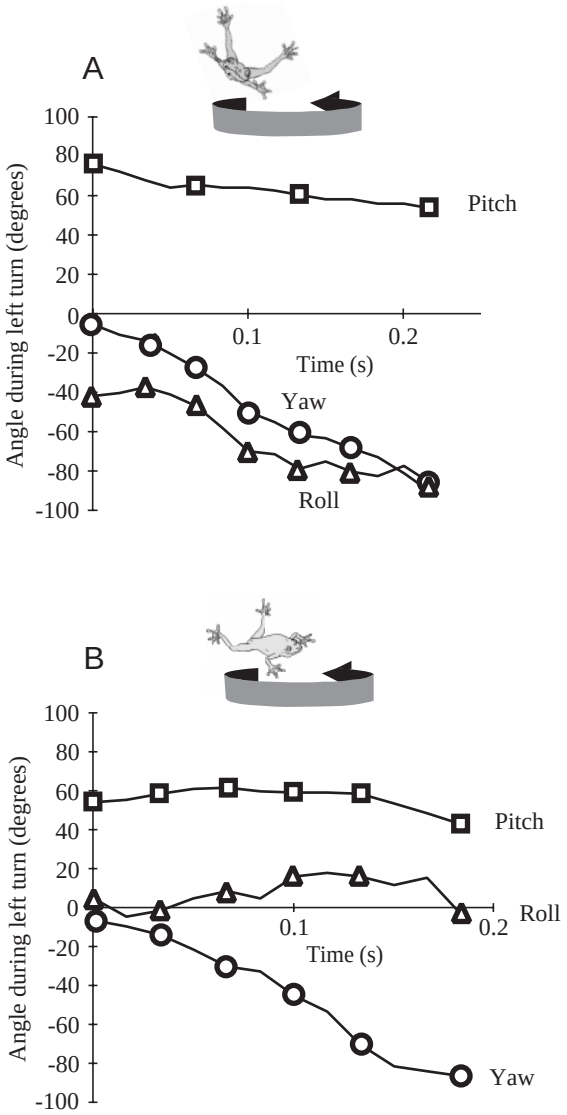

Fig. 7. Comparisons of rotation angles during two left turns. The angles of rotation about the pitch (nose up and down), roll (twisting about the cranial–caudal axis) and yaw (nose left and right) directions are shown for two typical left turns. (A) A banked turn performed by the frog with its hind feet held at the same vertical height above its body. (B) A 'crabbed' turn to the left performed by a frog with its right hind foot held higher than its left hind foot above the body. The patterns shown by the pitch angle and yaw angle are comparable between the two turns. However, the roll angle for the banked turn is between –40 ° and –60 ° compared with a roll angle of less than 20 ° for the 'crabbed' turn.

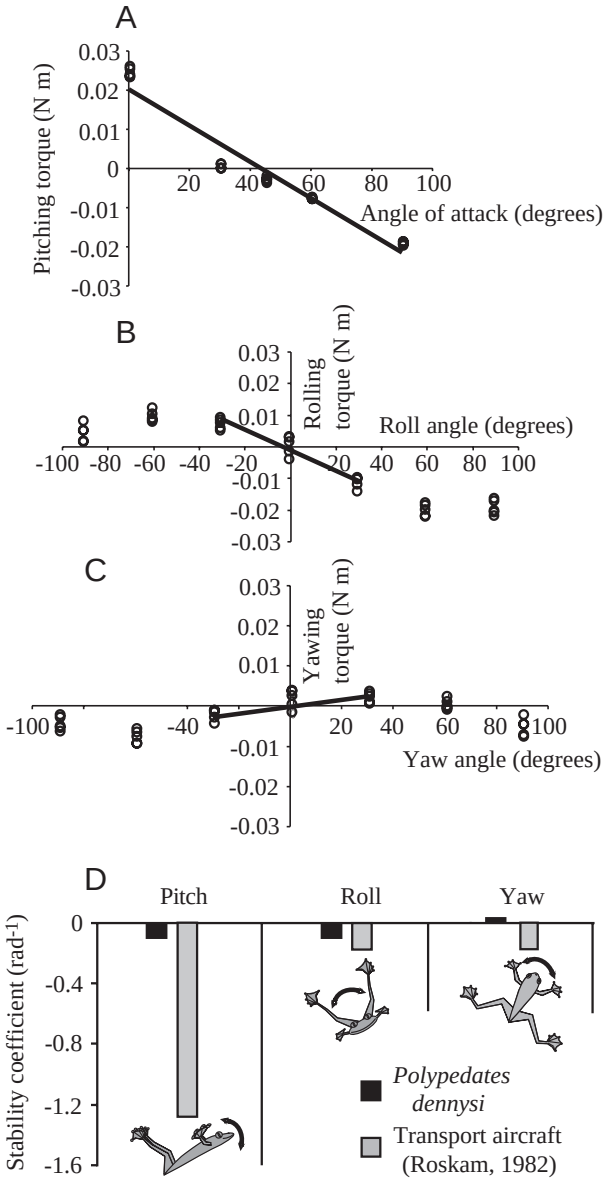

Fig. 8. Aerodynamic torques measured on a full-scale physical model of *Polypedates dennysi* posed in the gliding posture observed during non-maneuvering gliding. Aerodynamic torques about the pitch (A), roll (B) and yaw (C) axes are shown plotted against angle of attack, roll angle and yaw angle, respectively. Lines shown on each graph are linear regressions of the data. The linear regressions of rolling and yawing torque are taken over smaller ranges of roll angle and yaw angle, respectively, than the linear regression for pitching torque; the smaller range of angles reflects the lower level of perturbations in roll and yaw angle during gliding and is consistent with aeronautical engineering practice (McCormick, 1976). (D) Summary of aerodynamic stability coefficients (see text for definitions of coefficients) about the pitch, yaw and roll axes. Stability about a given axis is denoted by negative values, and instability is denoted by positive values. At the gliding speed (13 m s^{-1}) and angle of attack (45 °) used by *P. dennysi*, the frogs are slightly stable about the pitch axis and roll axes, and slightly unstable about the yaw axis.

mechanism (Emerson and Koehl, 1990). The scarcity of previous reports of animals using the crabbed turn mechanism begs the question: why do tree frogs utilize the crabbed turning mechanism?

The calculated maneuverability indices provide insight into the mechanical consequences of utilizing a banked turning technique as opposed to a crabbed turning technique. The maneuverability index of a frog using a banked turning technique is only slightly higher than that of a frog using a crabbed turning technique. This is because the frog's morphology produces only marginally more aerodynamic lift

than centripetal force. In contrast, a falcon, with a morphology considerably better suited to produce aerodynamic lift, has a maneuverability index for banked turns that is as much as three times higher than that of a frog.

In addition, frogs and birds use gliding in very different ways. Birds often glide while foraging, using thermals or wind currents to remain aloft for extended periods with little metabolic energy expended for flight. Frogs glide while travelling down from the canopy to mating sites on the forest floor (Roberts, 1994) and to escape predators (Stewart, 1985; Scott and Starrett, 1974). For birds, low-drag flight is of importance since aerodynamic drag reduces the time aloft while gliding. Frogs have not been observed actively decelerating prior to landing (Roberts, 1994), so minimizing gliding speed by gliding with relatively high aerodynamic drag would reduce the frog's impact speed when landing.

Much less additional aerodynamic drag is induced by turning using a banked turn compared with turning using a crabbed turn (McCormick, 1976). Thus, for birds, gliding using banked turns allows the bird to stay aloft longer because aerodynamic drag is lower than if the bird turned using a crabbed turn. For tree frogs, the potentially higher drag of crabbed turns will reduce gliding speed and, thus, reduce landing impact speed.

Stability

As discussed above, the passive aerodynamic stability of an animal directly affects the magnitude and rate of postural adjustments required to maintain a desired glide path in the presence of random disturbances such as wind gusts, but also adversely affects the maneuverability of the animal. Previous investigators posited that an evolutionary lineage that develops the ability to glide starts primitively as a glider that is passively stable and then gradually loses passive aerodynamic stability as each successive species' nervous system develops and refines the postural control necessary to stabilize actively (Maynard-Smith, 1952; Caple et al., 1983). Implicit in this hypothesis is the assumption that a stable glide path is an extremely important aspect of gliding. Some investigators who have studied the development of flight in lineages such as insects (Wootton and Ellington, 1991) and bats (Norberg, 1985) assume passively stable gliding to be an initial step towards developing the ability to glide.

Because frogs as a group are known more for their jumping ability than for their gliding ability, one would predict that gliding frogs should possess strong passive aerodynamic stability. One possible reason that gliding tree frogs are not highly stable is that the canopy environment through which frogs glide may be relatively sheltered from winds (Monteith and Unsworth, 1990; Campbell, 1977), so that tree frogs may rarely encounter random disturbances to their direction of flight due to wind gusts. Thus, aerodynamic stability may never have been of ecological importance to gliding tree frogs.

This manuscript was improved greatly by the comments of my advisor, M. A. R. Koehl, Jake Socha and two anonymous referees. Thanks also to Tim Cooper for his limitless technical expertise, and to my wife Mary, a source of constant inspiration. This research was funded by the University of California's Continuation of Research grant, by a Grant-in-Aid for Research from Sigma Xi and by National Science Foundation grant OCE-9907120 to M. A. R. Koehl.

References

Campbell, G. S. (1977). *An Introduction to Environmental Physics*. New York: Springer-Verlag.

Caple, G., Balda, R. P. and Willis, W. R. (1983). The physics of leaping animals and the evolution of pre-flight. *Am. Nat.* **121**, 455–476.

Carpenter, F. M. and Richardson, E. J. (1985). The geological record of insects. *Annu. Rev. Earth Planet. Sci*. **13**, 297–314.

Duellman, W. E. (1970). *The Hylid Frogs of Middle America*, vol. I. *Monograph of the Museum of Natural History*, pp. 87–130. Lawrence, KS: The University of Kansas.

Emerson, S. B. and Koehl, M. A. R. (1990). The interaction of behavioral and morphological change in the evolution of a novel locomotor type: 'flying' frogs. *Evolution* **44**, 1931–1946.

Emerson, S. B., Travis, J. and Koehl, M. A. R. (1990). Functional complexes and additivity in performance: a test case with 'flying' frogs. *Evolution* **44**, 2153–2157.

Emmons, L. H. and Gentry, A. H. (1983). Tropical forest structure and the distribution of gliding and prehensile-tailed vertebrates. *Am. Nat.* **121**, 513–524.

Harris, J. E. (1936). The role of fins in the equilibrium of the swimming fish. I. Wind tunnel tests on a model of *Mustelus canis* (Mitchill). *J. Exp. Biol.* **13**, 476–493.

Kingsolver, J. G. and Koehl, M. A. R. (1994). Selective factors in the evolution of insect wings. *Annu. Rev. Ent*. **39**, 425–451.

Maynard Smith, J. (1952). The importance of the nervous system in the evolution of animal flight. *Evolution* **6**, 127–129.

McCormick, B. W. (1976). *Aerodynamics, Aeronautics and Flight Mechanics*. New York: John Wiley & Sons.

Monteith, J. L. and Unsworth, M. H. (1990). *Principles of Environmental Physics*. New York: Routledge, Chapman & Hall, Inc.

Norberg, U. M. (1985). Evolution of vertebrate flight: an aerodynamic model for the transition from gliding to active flight. *Am. Nat.* **126**, 303–327.

Norberg, U. M. (1994). Wing design, flight performance and habitat use in bats. In *Ecological Morphology: Integrative Organismal Biology* (ed. P. C. Wainwright and S. M. Reilly), pp. 205–239. Chicago: University of Chicago Press.

Padian, K. and Chiappe, L. M. (1998). The origin and early evolution of birds. *Biol. Rev.* **73**, 1–42.

Pennycuick, C. J. (1968). A wind tunnel study of gliding flight in the pigeon, *Columba livia. J. Exp. Biol.* **49**, 509–526.

Pennycuick, C. J. (1972). Soaring behaviour and performance of some East African birds, observed from a motor glider. *Ibis* **114**, 178–218.

Roberts, W. E. (1994). Explosive breeding aggregations and parachuting in a Neotropical frog, *Agalychnis saltator* (Hylidae). *J. Herpetol.* **28**, 193–199.

Roskam, J. (1982). *Airplane Flight Dynamics and Automatic Flight Controls*. Lawrence, KS: Roskam Aviation and Engineering Corporation.

Scott, N. J. and Starrett, A. (1974). An unusual breeding aggregation of frogs, with notes on the ecology of *Agalychnis spurrelli* (Anura: Hylidae). *Bull. S. Calif. Acad. Sci*. **73**, 86–94.

Stewart, M. M. (1985). Arboreal habitat use and parachuting by a subtropical forest frog. *J. Herpetol.* **19**, 391–401.

Thewissen, J. G. M. and Babcock, S. K. (1992). The origin of flight in bats – to go where no mammal has gone before. *Bioscience* **42**, 340–345.

Tucker, V. A. and Heine, C. (1990). Aerodynamics of gliding flight in a Harris' hawk, *Parabuteo unicinctus. J. Exp. Biol.* **149**, 469–489.

Tucker, V. A. and Parrott, G. C. (1970). Aerodynamics of gliding flight in a falcon and other birds. *J. Exp. Biol.* **52**, 345–367.

Vogel, S. (1994). *Life in Moving Fluids: The Physical Biology of Flow*. Princeton, NJ: Princeton University Press.

Wootton, R. J. (1981). Palaeozoic insects. *Annu. Rev. Ent*. **26**, 319–344.

Wootton, R. J. and Ellington, C. P. (1991). Biomechanics and the origin of insect flight. In *Biomechanics in Evolution* (ed. J. M. V. Rayner and R. J. Wootton), pp. 183–212. Cambridge: Cambridge University Press.